Structure, Dynamics, and Reactivity in Hemoglobin

Joel M. Friedman

Summary. The static structure of hemoglobin and its functional properties are very well characterized. It is still not known how energy is stored and used within the structure of the protein to promote function and functional diversity. An essential part of this question is understanding the mechanism through which the overall protein structure (quaternary structure) couples to the local environment about the oxygen binding sites. Time-resolved resonance Raman spectroscopy has been used to probe the vibrational degrees of the freedom of the binding site as a function of protein structure. Comparison of the spectra from both equilibrium and transient forms of deoxy hemoglobin from a variety of mammalian, reptilian, and fish hemoglobins reveals that for each quaternary structure there exist two tertiary states stabilized by the presence or absence of an iron-bound ligand. Pulse-probe Raman experiments show that for photodissociated, ligated hemoglobins the local tertiary structure relaxes at a solution-dependent rate extending from tens of nanoseconds to microseconds. In this local environment, the linkage between the iron and the proximal histidine proves to be the single observed structural feature that responds in a systematic and substantial manner to structural changes in the protein. The additional finding of a correlation between the frequency of the iron–proximal histidine stretching motion (ν_{Fe-His}) and various parameters of ligand reactivity, including geminate recombination, implicates the associated localized structural element in the mechanism of protein control of ligand binding. On the basis of these and related finds, a model is presented to account for both coarse and fine control of ligand binding by the protein structure.

Much of biological research seeks to understand the nature of functional and structural diversity within a group of organisms. Comparative anatomy, physiology, and biochemistry all reflect the pursuit of this goal, each on its own scale. On the molecular level, proteins such as cytochrome oxidase or cytochrome c are readily identifiable within a group of organisms such as the vertebrates, regardless of the source. Despite structural similarities in a given protein from different sources, functional properties typically display significant variations. It is of fundamental importance to understand the structural or mechanistic basis for the functional diversity within a given protein, but, because so little is known about the inner workings of most proteins, such comparative biophysical studies are not generally feasible. Hemoglobin is one of the few exceptions.

Hemoglobin (Hb) is the primary oxygen-transport protein in virtually (*1*) all vertebrate organisms. The myriad of environmental niches and metabolic demands associated with this group of animals is matched by the wide spectrum of oxygen-binding properties of the respective hemoglobins. Furthermore, the oxygen-binding properties of a given hemoglobin often respond dramatically to the ever-changing physiological milieu within the organism. For example, the intrinsic oxygen affinity of a hemoglobin can vary by several orders of magnitude depending upon the oxygen concentration. This phenomenon gives rise to the sigmoidal O_2 saturation curve indicative of a cooperative binding process—the more oxygen that is bound, the higher the oxygen affinity of the remaining unbound sites. Solution conditions such as *p*H and phosphate concentration further modulate the binding properties of given hemoglobins. What is intriguing is that in all the above cases the oxygen-binding site is the same iron porphyrin or heme, and yet there is a very broad spectrum of ligand binding properties as a function of both animal source and solution conditions. Clearly, variation in the protein matrix surrounding the heme must be responsible for this variety. This article addresses the question of whether this broad spectrum arises out of some specific linkage through which changes in protein structure are communicated to the oxygen binding sites in some functional sense.

Typical hemoglobins are tetrameric proteins consisting of two α subunits and two β subunits. Each subunit has an oxygen-binding site. The coarse control of oxygen binding in hemoglobin has been described within the context of a two-state allosteric model (*2*, *3*). Within this description there is an O_2 concentration–dependent equilibrium between two distinct quaternary structures of the protein. At low O_2 concentration S, when the hemoglobin is primarily deoxygenated, the low-affinity tense or T-state quaternary structure is favored. Increasing the O_2 pressure and hence the degree of saturation shifts the equilibrium to the high-affinity relaxed or R-state structure. Fine tuning of this mechanism occurs through solution-dependent and species-specific modulation of both this equilibrium and the ligand-binding properties of a given quaternary structure (*4*). The question therefore becomes one of understanding how the genetic- and solution-induced differences in protein structure associated with the coarse and fine control of ligand binding are manifested at, or communicated to, the localized ligand binding sites.

A general approach to this question is to establish which structural degrees of freedom of the binding site are responsive to protein structure. Subsequently it must be determined which of these structure-sensitive features correlate with reactivity. X-ray crystallographic studies have revealed two distinct configurations associated with the interface between the subunits (*5*). The two protein structures resulting from these two observed interfacial geometries are the two accessible quaternary structures for Hb. In the x-ray study it was also observed that the protein structure about the heme within each subunit (tertiary structure) changes in switching from the deoxy T state to the carboxy R state of Hb.

From the x-ray study it is not possible to determine to what extent these tertiary structure differences originate from a pure R-T–induced change or from a ligation-induced difference. Furthermore, these studies do not provide a means of discerning which of the differences in the tertiary structure are perturbing the oxygen-binding site in a functional sense. It

The author is at AT&T Bell Laboratories, Murray Hill, New Jersey 07974.

is therefore desirable to systematically probe the binding site, that is, the heme, in a manner that reveals what is changing as a function of both state of ligation and quaternary state as well as which structural features correlate with ligand binding properties. Since the binding of a ligand significantly perturbs the electronic and nuclear structure of the iron porphyrin, the anticipated subtle protein-induced effects upon the heme are not likely to be observed in a comparison of a deoxy and a ligated Hb. Instead, we require the hemes in all the comparisons to be in the identical electronic state. This requirement is accomplished by comparing R- and T-state varieties of both equilibrium deoxy forms of Hb and transient deoxy species derived from photodissociated ligated Hb's. Earlier studies have shown that photodissociation and subsequent electronic relaxation to a ground-state deoxy (high-spin Fe^{+2}) heme occurs on a time scale of ≤ 5 psec (*6–10*), whereas appreciable or detectable protein relaxation does not appear to occur until at least many tens of nanoseconds after photodissociation (*11, 12*). Consequently, the transient species occurring within 10 nsec of photolysis typically consist of deoxy hemes surrounded by a protein matrix that has the tertiary structure associated with the fully ligated parent species. Therefore, by spectroscopically comparing both R- and T-state varieties of deoxy and transient deoxy Hb's, it should be possible to distinguish the induced changes in the tertiary structure influencing the heme-associated degrees of freedom that originate from either ligation or change in the quaternary structure.

Transient absorption studies have very effectively revealed the kinetics associated with the relaxation of the photo-induced ligand-free transient species of Hb. On the microsecond time scale, such studies (*13*) have revealed the rates of change of the quarternary structure subsequent to the photolysis of R-state, ligated Hb's. Similar absorption studies (*12, 14*) and transient Raman study (*11, 15*) in the nanosecond time scale have revealed relaxation dynamics ascribable to changes in the tertiary structure occurring prior to the R-T switch. Because the intrinsically broad absorption spectra of these molecules contain little structural information, they cannot be used to extract information about what specifically is changing with time. Even a clear distinction between tertiary and quaternary relaxation is not unambigous when the porphyrin absorption is used as a probe. Alternatively, the resonance Raman spectra of the heme is well characterized with respect to numerous porphyrin-associated degrees of freedom (*16, 17*). In addition, the frequencies of several Raman bands originating from both stable and transient deoxy forms of Hb have been characterized with respect to features of the tertiary structure that are responsive to the quaternary structure or the state of ligation immediately (nanoseconds) prior to the excitation pulse (*15, 18–21*). The frequencies of some of these protein-sensitive Raman bands have been shown to correlate with ligand reactivity (*15*). For these reasons Raman scattering provides a nearly ideal probe of structure with which to address questions concerning functional communication between the heme and the protein.

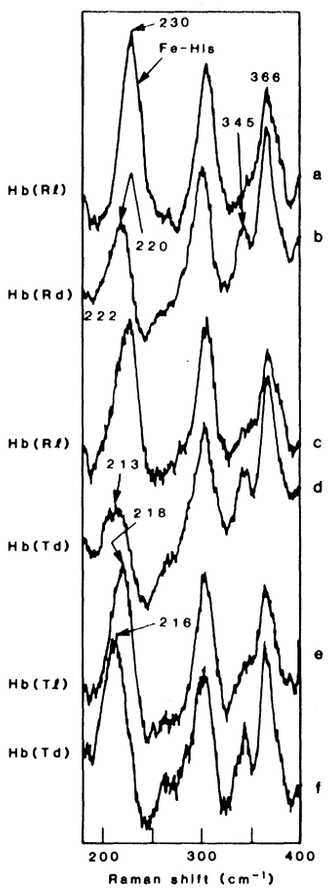

Fig. 1. A comparison of the low-frequency resonance Raman spectra of equilibrium and transient forms of deoxy Hb from three different animal sources. The transient deoxy species were generated and probed by photodissociating the carboxy form of the protein with a single 10-nsec pulse (1 mJ, 10 Hz) at 4350 Å. Experimental details can be found elsewhere (*15, 20–23, 34*): (a) photolyzed COHb (Kempsey), *p*H 9.0; (b) deoxy Hb (Kempsey), *p*H 9.0; (c) photolyzed COHb (loggerhead sea turtle), *p*H 7.5; (d) deoxy Hb (loggerhead sea turtle), *p*H 7.0; (e) photolyzed COHb (tuna), *p*H 5.8; (f) deoxy Hb (tuna), *p*H 7.5. The designations on the left indicate the tertiary structure of the starting material.

Tertiary Structure

In Raman studies it was observed that the quaternary structure affected those vibrational frequencies (for example, ν_4) known to be sensitive to the π electron distribution of the porphyrin macrocycle (*22, 23*). Comparisons between deoxy T-state and deoxy R-state equilibrium species revealed a systematic decrease in the frequency of these π-sensitive modes. The transient Raman studies showed that within each quaternary structure ligand binding induces a tertiary reorganization that further decreases these frequencies from the equilibrium deoxy value. It was concluded from these studies that the electron density in the lowest π^* orbitals, due primarily to back-bonding through the iron, increased in the following sequence: deoxy T, photolyzed ligated T, deoxy R, and photolyzed ligated R. These studies indicate the existence of two distinct tertiary configurations within each of the quaternary structures: one in quasi-equilibrium with the deoxy heme and the other with the ligated heme. Thus with regard to the heme environment (heme pocket), there appear to be four possible spectroscopically detectable configurations: Hb(Td), Hb(Tℓ), Hb(Rd), and Hb(Rℓ), corresponding to the T-state deoxy, T-state ligated, R-state deoxy, and R-state ligated heme pocket configurations, respectively. Because both peripheral and axial perturbations of the heme can cause shifts in ν_4 (*24*), it is necessary to turn to other regions of the Raman spectrum to obtain more detailed structural information about these four tertiary states.

A comparison of the low-frequency region of the Raman spectra of deoxy HbA and photolyzed carboxyhemoglobin A (COHbA) at 10 nsec reveals two very prominent changes. The frequency of the Raman band associated with the stretching motion between the iron and the proximal histidine (ν_{Fe-His}) increases from 215 to 230 cm^{-1} in going from the equilibrium species to the transient. In addition, the well-defined peak at 345 cm^{-1} shifts in the transient to ~355 cm^{-1}, where it is discernible as a weak shoulder on the low-frequency side of the invariant 360-cm^{-1} peak. In deoxy HbA, the heme pocket configuration is Hb(Td) whereas in the transient it is initially Hb(Rℓ); consequently, a companion of these two deoxy species involves a change in the tertiary structure due to both quaternary state and ligation. It is therefore not possible to state whether these changes are due to the R-T difference or to the fact that one was initially ligated. To separate out these

two possible contributions, I have examined a variety of hemoglobins including those that can be stabilized in either the R or T state for both ligated and deoxy proteins (see Fig. 1).

Comparative studies reveal that the changes observed for the 345-cm^{-1} peak are independent of quaternary state. Instead, the position of this band reflects the recent history of the heme with respect to ligation. It appears that a spectrum that has a distinct 345-cm^{-1} peak is characteristic of a heme pocket having either the Hb(Td) or the Hb(Rd) tertiary structure. Alternatively, a spectrum of deoxy heme that has only the 355-cm^{-1} shoulder reflects a heme pocket that retains at least some memory of a ligated configuration, that is, Hb(Tℓ) or Hb(Rℓ). Similar conclusions were reached from Raman studies on Hb at cryogenic temperatures (*25*).

The Iron–Proximal Histidine Linkage

The tertiary structure as reflected in iron–proximal histidine stretching motion (ν_{Fe-His}) responds both to the quaternary structure and to the state of ligation. This behavior is reminiscent of that observed for the previously discussed high-frequency π electron–sensitive modes (for example, ν_4). Indeed, studies on both equilibrium deoxy and transient deoxy Hb's reveal an inverse linear correlation between ν_4 and ν_{Fe-His} (*18, 19*). Such a finding is consistent with modulation of the π electron density in the porphyrin macrocycle by changes associated with the iron–proximal histidine linkage (*2*). In summary, the general pattern for ν_{Fe-His} as determined from continuous wave and time-resolved studies is that this frequency increases in going from HB(Td) to Hb(Rd), from Hb(Td) and Hb(Tℓ), and from Hb(Rd) to Hb(Rℓ), with Hb(Tℓ) having approximately the same or slightly lower frequency range as Hb(Rd).

Within each category of tertiary structure (for example, Rℓ) there is a range of values for ν_{Fe-His} that is determined by both animal source and solution conditions (see Fig. 2). Related species tend to have similar values for ν_{Fe-His}. Sea turtles, freshwater turtles, and mammals appear to have distinctive values for ν_{Fe-His}. In general, the addition of inositol hexaphosphate (IHP) at low *p*H decreased ν_{Fe-His} in the nanosecond transients; however, the extent of this decrease is species-specific. For some hemoglobins [fish, turtle, and snake (*Acrochordus*)] this decrease is consistent with an actual shift in the equilibrium from a population of Hb(Rℓ) structures to one with a substantial contribution from Hb(Tℓ) structures. The shift in ν_{Fe-His} with IHP for most mammalian hemoglobins indicates that IHP distorts the Rℓ structure toward Tℓ but the quaternary structure still remains R. From the above findings it is clear that ν_{Fe-His} reflects some local structural feature at the binding site that is strongly modulated by protein structure. Ligand binding induces a structural change that is modulated on a coarse level by the quaternary structure, and this in turn is further tuned by solution conditions and evolution (that is, animal type).

A correlation between ν_{Fe-His} and ligand binding is suggested by the observation that ν_{Fe-His} is responsive to perturbations of protein structure that are known to alter reactivity. In switching from the T-state to the R-state quaternary structure the affinity for oxygen typically undergoes a sizable increase as does the value for ν_{Fe-His}. Within the R state there is a range of values associated with ν_{Fe-His} for the photolyzed material. For every comparison between high *p*H and low *p*H, the lower ν_{Fe-His} value is associated with the low *p*H conditions favoring a decreased oxygen affinity in cases where the quaternary structure both does not and does change with *p*H [for example, HbA versus Hb (tuna)]. Furthermore, for fixed solution conditions the species-specific distribution of values for ν_{Fe-His} increases with affinity within a given quaternary state. For example, at *p*H 8.0 the low-affinity sea turtle hemoglobins (*26*) have the lowest ν_{Fe-His} of any of the photolyzed R-state COHb (see Fig. 2), whereas the high-affinity hemoglobins are at the high end for ν_{Fe-His}. Other studies show a correlation between ν_{Fe-His} and the equilibrium binding constant (K_1) for equilibrium deoxy Hb's (*27*). Despite this relation, it is difficult to analyze this suggested correlation in detail because oxygen affinity is a property of a bulk solution with many contributing structures. Instead, what is needed is a parameter of ligand reactivity that can be associated with spectroscopically well-defined tertiary configurations.

Geminate Recombination

Frauenfelder and his co-workers (*28, 29*) have used cryogenic studies to probe the dynamics of ligand binding in hemoproteins. Their studies indicate that by lowering the temperature it is possible to isolate several sequential steps associated with ligation dynamics. Below a certain temperature, a photodissociated ligand remains trapped within the parent protein. Subsequent rebinding occurs only from this protein-trapped population. For solutions at ambient temperatures, the rapid rate of ligand escape into the surrounding aqueous solvent makes the rate of this geminate rebinding process too fast to permit detection by the standard microsecond techniques. Using nanosecond laser pulses for excitation, several groups independently detected and reported geminate recombinations in Hb occurring over an approximately 100-

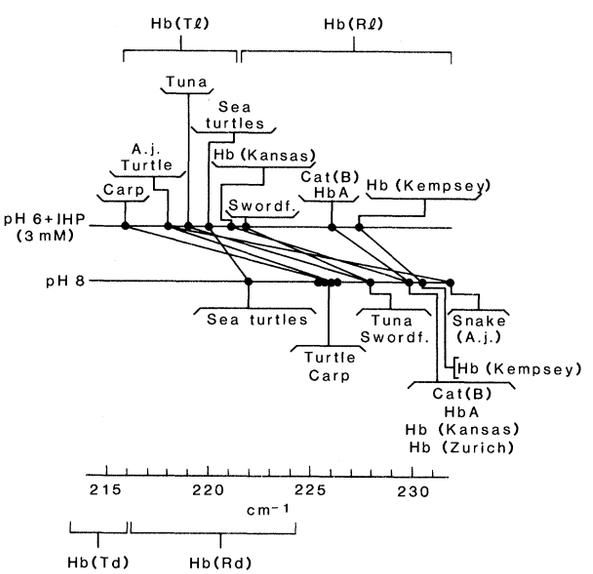

Fig. 2. The values of ν_{Fe-His} from transient forms of deoxy Hb (Hb*) derived from different animal sources under high and low *p*H conditions. In all cases shown Hb* is the transient occurring within 10 nsec of photodissociation of the parent carboxy protein. The range of values of ν_{Fe-His} for equilibrium and transient forms of the R- and T-state deoxy Hb's are also shown. Abbreviations: A.j., *Acrochordus javanicus* (elephant trunk snake); swordf., swordfish. Under the category of turtle are included five different species of freshwater turtles; the category of sea turtle includes the green, leatherback, loggerhead, and Kemp's Ridley sea turtles. Details regarding the comparative physiology and behavior of these animals in so far as they affect respiration can be found in (*45*).

nsec time course (*30, 31*). Subsequent picosecond absorption studies revealed ligand-specific geminate processes occurring on subnanosecond time scales (*7, 8, 32*). These fast and slow geminate processes appear to correspond to the two internal rebinding processes observed in the frozen samples, binding from the heme pocket (process I) and binding from the protein matrix (process M), respectively. Thus we have a ligand-binding process occurring on a time scale that is faster than the switching time for the quaternary structure ($\geq$10 μsec) and the tertiary relaxation within a given quaternary state (<1 μsec). Consequently, if one assumes that bond formation and rupture between the ligand and the heme occurs faster than any of the above structural relaxations, then it is possible to analyze the geminate recombinations process associated with a specific tertiary structure of a given hemoglobin.

For any spectroscopically identifiable tertiary structure it is now possible to associate a reaction coordinate diagram which describes the dynamics and binding properties of an intraprotein ligand in the vicinity of a heme (*15*) (see Fig. 3). There is evidence that, upon photoinduced ligand dissociation, the heme relaxes from a planar six-coordinate, low-spin heme to a five-coordinate, high-spin deoxy heme in less than a picosecond regardless of the surrounding protein matrix (*10*). Cryogenic temperatures do not appear to impede this relaxation (*33*). Consequently, at essentially the instant of ligand dissociation, there is a deoxy heme with the nearby ligand surrounded by a heme pocket matrix having a tertiary structure that is basically that of the parent ligated species but with the slight changes necessary to accommodate the nonplanar deoxy heme (well B in Fig. 3) (*34*). The ligand can either rebind or diffuse into the bulk protein. This process is associated with the subnanosecond events. From cryogenic studies (*35*) and because ligand diffusion appears to be rather insensitive to differing protein structures (*36*), it is assumed that variation in barrier I and in the depth of well A (Fig. 3) determine the relative yield of this process for given solution conditions. Once outside the heme pocket (well C), the geminate rebinding rate is determined largely by a diffusion-controlled process that gives rise to the observed 100-nsec rebinding. The various parameters regulating this process have been lumped into barrier II, which for the reason expressed above is not likely to be sensitive to changes in protein structure; nevertheless, the overall yield still depends upon the probability

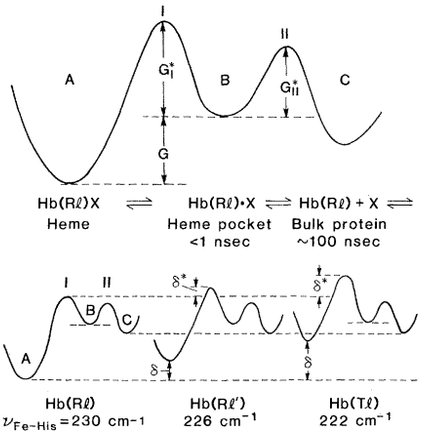

Fig. 3. The reaction coordinate diagram for geminate rebinding in Hb. In the top portion, the captions under the various potential wells indicate the location of the ligand X. For well A, the ligand is bound to the heme whereas for wells B and C the dissociated ligand is within the immediate vicinity of the heme (heme pocket) and the bulk protein, respectively. The approximate lifetimes of these two geminate configurations are also shown. The greater stability of well C over well B is assumed to be due to an increase in entropy associated with the motional constraints of X. The bottom portion shows how this potential surface varies with the tertiary structure of a given heme pocket.

for rebinding at the heme, which is a function of barrier I and well A. Thus, for any tertiary configuration, such as Hb(Rℓ), a discussion of geminate rebinding for ligand X includes Hb(Rℓ)X, [Hb(Rℓ)·X], and [Hb(Rℓ) + X]—the ligated heme, the deoxy heme with the ligand in the heme pocket, and the deoxy heme with ligand in the bulk protein (Fig. 3). This description is very similar to that used by Frauenfelder and co-workers to describe processes I and M observed in photodissociated ligated hemeproteins at cryogenic temperatures (*28, 35*).

Within this working model, protein-induced variations in reactivity are a result of changes in either the depth of well A, the height of barrier I, or both. There are several indications that geminate recombination is sensitive to changes in protein structure. Macroscopic parameters of reactivity such as on and off rates are known to be responsive to the structure of the protein. For example, large differences are observed for the two quaternary structures of hemoglobin. These processes depend on ligand diffusion, bond formation (or rupture), and geminate binding. Because diffusion of diatomic ligands through proteins is essentially insensitive to changes in protein conformation (*36*), the variations in these macroscopic parameters with structure originate from the responsiveness of both the geminate recombinations and the intrinsic dissociation and association rates to protein structure.

Similarly, the protein-specific variation in the time-averaged quantum yields of photolysis for a given ligand have been ascribed to differences in the yields of geminate recombination rather than to any protein specificity in the electronically determined intrinsic quantum yields (*23*). For COHb and carboxymyoglobin (COMb) the observed quantum yields for photolysis averaged over at least 1 μsec are ~50 percent and >95 percent, respectively; these values closely match the observed respective yields for the 100-nsec geminate recombination (*31, 37*). The measured geminate recombination rates and yields were shown to indicate an essentially protein-insensitive rate for the escape of the ligand from the protein and a protein-sensitive rebinding rate (*37*). In comparing R- and T-state forms of ligated HbA, the averaged quantum yield was shown to significantly increase in going from R to T (*38*). Similar changes have been reported for the 100-nsec geminate process (*14*). On shorter time scales, it has been shown that the yield of photolysis averaged over the first 10 nsec subsequent to photodissociation is significantly affected by protein structural changes in oxy, carboxy, and nitroxy Hb's from a variety of upper and lower vertebrates (*15, 39*). Because the intrinsic photolysis for a given ligand appears insensitive to the protein matrix, these changes must originate from variations in the subnanosecond geminate recombination. These results are consistent with the idea that modulation of geminate recombination by protein structure occurs at the level of potential well A and barrier I (Fig. 3). My question concerning the relation between structure and reactivity now focuses upon the possible correlations between specific structural parameters and changes in the depth of well A and the height of barrier I.

It has been observed that in a large variety of vertebrate Hb's a relation exists between shifts in the frequency of both ν_4 and ν_{Fe-His} and the yield of geminate recombination averaged over equivalent 10-nsec pulses (*15, 23, 39*). Solution conditions that effect a change in ν_{Fe-His} (or ν_4) are always associated with a change in this geminate yield. A decrease in ν_{Fe-His} correlates with an increase in the time-averaged photolysis yield which, for the reasons already mentioned, indicates a decrease in geminate recombination. In all of the above cases the comparison was between the same hemoglobin but under different so-

lution conditions. In all cases, regardless of ligand (NO or O_2), the T-state species exhibit the greater time-averaged yield over 10 nsec. Similarly in comparisons of R-state oxy and carboxy human Hb's (mutant, chemically modified HbA and HbA) the magnitude of the shift in ν_{Fe-His} upon lowering the *p*H and adding IHP (see Fig. 2) correlates with the increase in photolysis yield. The emerging picture is that the B to A (Fig. 3) gemi nate process (process I) decreases with decreasing ν_{Fe-His}. Thus, if other degrees of freedom that influence reactivity are not changing, the subnanosecond geminate yield is expected to decrease with changing tertiary structure in the following sequence Hb(Rℓ), Hb(Rℓ'), and Hb(Tℓ), where Hb(Rℓ') is the *p*H + IHP–modified ligated R state (see Fig. 3).

Experiments on Hb (Zurich) (HbZ) indicate that variations in structural parameters other than those associated with ν_{Fe-His} can also be important in controlling process I. In the β subunit of HbZ the distal histidine is replaced by an arginine. The result is a more open, less constrained heme pocket on the distal side. It has been shown from the temperature dependence of the geminate rebinding rates for CO in frozen solutions that barrier I for the mutant subunits is indeed lower than in normal β chains (*29*). A similar conclusion was reached when transient Raman was used to monitor the 10-nsec averaged photolysis yield as a function of temperature (40 to 250 K) for COHbA and COHbZ (*39*). Transient Raman studies (*39*) also show that this distal perturbation does not alter either ν_{Fe-His} or the response of ν_{Fe-His} to IHP. However, under these conditions HbZ consistently exhibits a greater yield of geminate rebinding (measured over 2.4 nsec) than HbA. These and earlier (*40*) results indicate that the distal environment about the heme establishes a baseline height for barrier I that is then modulated by protein-induced changes on the proximal side as reflected in ν_{Fe-His}.

On the basis of the perturbation scheme of Traylor and co-workers (*41*), the distal perturbation of the kind seen in HbZ is associated with an equivalent decrease in barrier I and well A. In that scheme the binding of CO requires a configurational change in the distal heme pocket which equivalently modifies the energy of both the transition state for barrier I and the ligated state A. In HbZ this change in configuration is reduced relative to HbA, resulting in an equivalent decrease in barrier I and well A ($\delta = \delta^*$ in Fig. 3). On the basis of this description of the distal effect, there should be little if any difference in the intrinsic spontaneous dissociation rates for COHbA and COHbZ at the same *p*H. In contrast to the distal effect, proximal perturbations alter the transition state to the degree that it resembles the final ligated state. Consequently, δ^* will always be less than δ. It has been suggested that the properties of the transition state can account for the ligand-specific response of the on and off rates to quaternary structure (*42*). The fast-binding ligands such as NO and O_2 have $\delta^* << \delta$, whereas slow-binding CO has δ^* approaching δ.

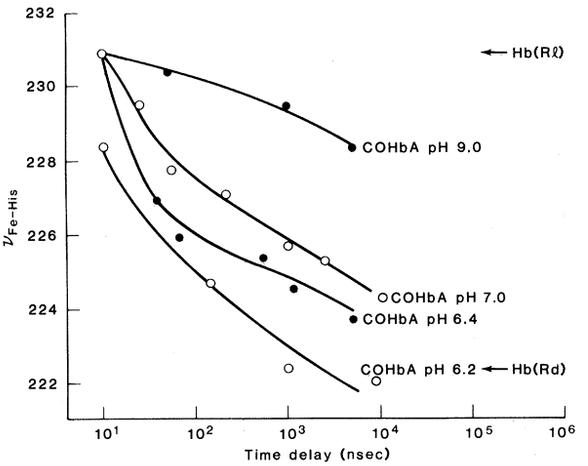

Fig. 4. The time evolution of ν_{Fe-His} in photodissociated COHbA as a function of solution conditions. The upper and lower arrows on the right side indicate the values of ν_{Fe-His} associated with the ligated R-state [Hb(Rℓ] and deoxy R-state [Hb(Rd)] tertiary configurations, respectively. The low-*p*H solutions also contained approximately 1 m*M* IHP. The experiments were conducted at 35°C to minimize the effects upon the spectral evolution due to geminate recombination.

Structural Relaxation

Up to this point, I have considered the dynamics of ligands confined to a protein having a fixed average configuration. Whereas this fixed configuration description is probably accurate for process I in Hb under most conditions, longer processes ranging from the 100 nsec geminate process to the events contributing to the macroscopic on and off rates may involve a protein configuration that is evolving. As discussed earlier, there is a ligated and deoxy tertiary structure associated with each quaternary state. These two tertiary configurations are readily distinguished by the use of the Raman spectrum (*15, 34*). The change from one tertiary configuration to the other within the same quaternary state is typically associated with a change in ν_{Fe-His}. Because a change in ν_{Fe-His} indicates a change in well A and barrier I, it is important to determine the rate at which the tertiary structure and hence ν_{Fe-His} evolves subsequent to ligation or deligation. With the use of nanosecond pulse probe techniques with a variable delay, it has been shown (*15, 34, 43*) that subsequent to photodissociation by a 10-nsec pulse the Hb(Rℓ) configuration relaxes to the Hb(Rd) configuration at a solution-dependent rate (see Fig. 4). From the time scale, the values of ν_{Fe-His} and the behavior of the peak at 345 to 355 cm^{-1} it is clear that this decay reflects the transition from Hb(Rℓ) to Hb(Rd). It is seen that ν_{Fe-His} at 10 nsec is the same over a large range of *p*H values; nevertheless, within 100 nsec large differences are apparent. At low *p*H the structural relaxation is sufficiently rapid to indicate that ν_{Fe-His} is decreasing appreciably over the time scale of the 100-nsec geminate rebinding process. Thus it will not generally be possible to use a single reaction coordinate diagram in the description of the slower geminate process or any of the macroscopic on or off rates as well.

The observation of this nanosecond and longer tertiary relaxation in Hb but not in Mb (*18*) indicates that in Hb in addition to the sequential ligand binding steps, a parallel process (*44*) is occurring that can also affect ligand binding (see Fig. 5). For a ligand to bind it must overcome several sequential potential energy barriers existing between the solvent and the heme. Upon ligand binding the tertiary structure begins to evolve. Within the R quaternary structure, for example, ligand binding initiates the change from the Rd to the Rℓ tertiary structure. The rate of tertiary structure change is solution- and species-dependent. Upon ligand dissociation the protein starts to relax back to the Rd structure.

The extent to which the structure reverts will depend upon the geminate rebinding since religation stops the relaxation toward Rd and reinitiates evolution toward Rℓ. Since both the geminate rebinding and the intrinsic ligand dissociation rate appear to depend upon the tertiary structure, the solution- and species-dependent rate of structure relax-

ation will have an effect upon the probability of achieving a ligated Rℓ species. For example, at low pH, when the ligand binds to a heme coupled to the Rd protein structure, the evolution toward Rℓ (k_3) is slow. Ligand dissociation is more probable for the Rd-like transient intermediate structures. Upon dissociation, geminate rebinding is also reduced both because the Rd environment is less favorable for rebinding and the rate of relaxation back to Rd (k_3') is enhanced at low pH. In contrast, at high pH, formation of the ligated Rℓ species is favored (k_3 fast, k_3' slow). Thus geminate rebinding is more probable and dissociation less probable relative to conditions that favor a distribution of structures toward the Rd end of the structural spectrum. In all instances where the tertiary relaxation is occurring in parallel to the sequential movements of the ligand, the longer the ligand remains off the heme, the less likely is the probability for rebinding. This feature imparts to the process a self-induced trapping quality in that upon dissociation the protein structure about the heme evolves at a solution-dependent rate to trap the deoxy heme by increasing the barrier for rebinding.

Temperature Effects

The observed decrease in ligand affinity with increasing temperature can be understood in terms of the above scheme. When a ligand undergoes spontaneous dissociation, the tertiary structure starts to relax. This relaxation is pH-dependent. Temperature changes affect the pK_a's (negative logarithm of the acid constant of various amino acids, which in turn modify the relaxation rates of the tertiary structure. Thus for a given interval over which a ligand remains off the heme, the tertiary structure relaxation will proceed at a temperature-dependent rate. The temperature also affects the diffusion of the dissociated ligand through the protein. As the temperature increases, the ligand is more likely to diffuse away from the heme after dissociation. The net affect is to increase the average interval over which the ligand remains away from the iron. The longer this interval, the greater the amount of relaxation, which makes subsequent rebinding less likely. At high pH, the tertiary relaxation subsequent to dissociation proceeds very slowly; as a result, the spectra reflecting the relaxation are not affected by temperature as much as in the low-pH samples. From the earlier analysis in this work it follows that the extent of relaxation from the end point ligated spectrum also reflects the average barrier height (I) and well depth (A) associated with ligand. The temperature alters the steady-state populations of Hb(Rd), Hb(Rℓ'), and Hb(Rℓ) by affecting k_3', k_3, and k_b' for the reason described above (see Fig. 4). An increase in Hb(Rℓ') and Hb(Rd) at the expense of Hb(Rℓ) indicates a decrease in the overall ligand binding affinity within the R quaternary state because k_a(Rℓ) > k_a(Rℓ') > k_a(Rd) and k_a'(Rℓ) < k_a'(Rℓ') < k_a(Rd). When the pH heavily favors the formation of a tight-binding Hb(Rℓ)X [k_a(Rℓ) large and k_a'(Rℓ) small] as in the case of oxy or carboxy HbA at pH 9, spontaneous dissociation is a low-probability event. Consequently, the ligated heme pocket tends to remain locked into the Hb(Rℓ) configuration over a wide range of temperature. At lower pH values the rate of spontaneous dissociation for oxy HbA increases, which increases the susceptibility of the system to temperature-dependent changes in k_3, k_3', and k_b' by generating a larger population of [Hb(Rℓ)·X]. Similarly the low intrinsic affinity of certain R-state Hb's (for example, sea turtles) even at pH 9 [k_a(Rℓ) small, k_a'(Rℓ) large] results in sizable and hence temperature-vulnerable population of [H6(Rℓ)·X]. It is possible that in such low-affinity Hg's a stabilization of the affinity against drastic temperature effects may be achieved by a slow, relatively pH-insensitive tertiary relaxation rate as has been observed for the loggerhead turtle (*45*). The addition of tight-binding ligands such as CO to any of these systems decreases the temperature effects by diminishing the population of [Hb(Rℓ)·X]. There are, however, Hb's from such organisms as the bluefin tuna (*46*) and possibly some sea turtles (*34, 45*) for which at certain pH values an increase in temperature increases the affinity by shifting the equilibrium further toward the R quaternary state. In contrast to the case for most Hb's at pH 7 in which an increase in temperature (2° to 30°C) produces a decrease in ν_{Fe-His} in the photolyzed spectrum of the oxyderivative, those from the bluefin tuna and the green sea turtle exhibit increases in ν_{Fe-His} (*34, 45*).

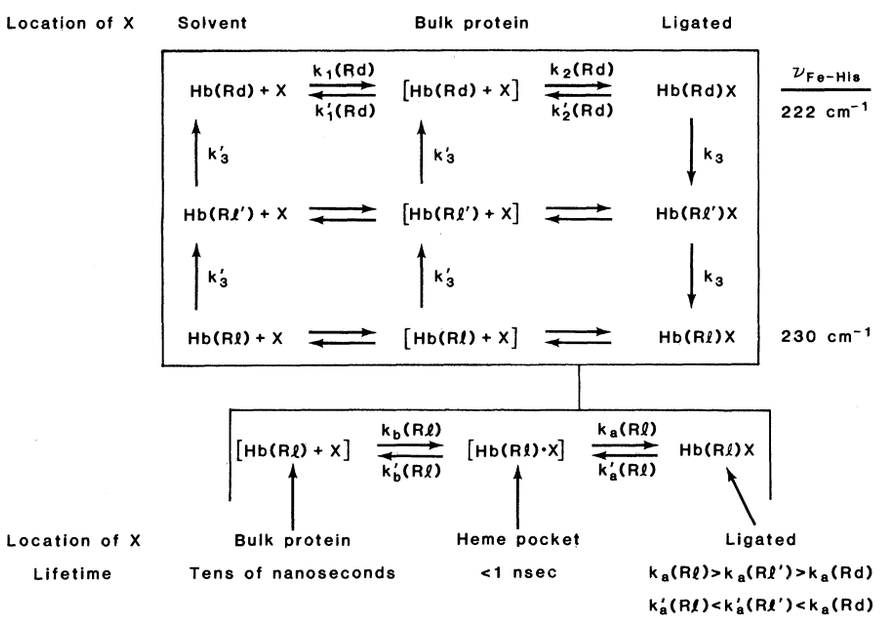

Fig. 5. Scheme for understanding solution-dependent variation in the ligation properties within the R quaternary state based upon spectroscopically identifiable intermediates. Instead of Hb* and ligated Hb the various deoxy and ligated hemes are identified according to the tertiary structure: Hb(Rd), Hb(Rℓ), and Hb(Rℓ') refer to deoxy hemes embedded in proteins having deoxy R, ligated R, and intermediate tertiary structures, respectively, while the corresponding ligated forms are designated by the same nomenclature but followed by an X. For example, Hb(Rd)X would be a ligated heme surrounded by the deoxy R tertiary structure. At the bottom of the figure is shown the breakdown of the processes that were lumped into the k_2 and k_2' steps within the box. The various k_2's refer to the overall geminate recombination associated with differing tertiary configurations. This process is broken down into the recombination derived from the bulk protein as well as from within the heme pocket. Modulation of the geminate process by the tertiary structure occurs at level k_a and k_a', which is related to the proximal histidine–controlled barrier I and well A of Fig. 3. On the right side of the figure are shown the values of ν_{Fe-His} associated with Hb(Rd) and Hb(Rℓ) derived from HbA. Sequential movement of the ligand is along the horizontal axis, whereas the structural changes occurring along the vertical axis are the parallel processes discussed in the text.

Structure and ν_{Fe-His}

The transient Raman studies discussed in this and other works indicate a close connection between changes in ν_{Fe-His} and regulation of ligand-binding proper-

ties. Clearly, it is of interest to explore the structural basis behind these associations. It has been proposed that the tilt or cant of the proximal histidine within its own plane with respect to the heme plane is a structural parameter that can be associated with the variation in ν_{Fe-His} (*15, 21*). Variations in the tilt angle and its potential importance in the mechanism of cooperative binding were first noted by Karplus and co-workers (*47*). We now expose the implications of this association. This tilt can affect the Fe–His bond by decreasing the separation between the imidazole carbon and the pyrrole nitrogen on the same side. A decrease in this distance increases the repulsive force between the imidazole and the heme, which weakens the Fe–His bond and causes a decrease in ν_{Fe-His} within the small tilt approximation. Thus for a fixed displacement of the iron, we associate a decrease in this Raman frequency with an increase in the histidine tilt. The frequencies observed in both steady-state and transient Raman studies indicate that, for comparisons of either the deoxy or transient deoxy species, the corresponding R-state Hb has a less tilted geometry (see Fig. 5).

Upon photodissociation of a ligated heme, the iron moves to an out-of-plane geometry within at most a few vibrational periods. This conclusion is based upon both theoretical studies, which show that for a five-coordinate heme the very sizable repulsive forces between the imidazole carbons and the pyrrole nitrogens are significantly reduced by the movement of the iron ~0.3 Å out of plane (*48*), and transient absorption results, which demonstrate that the subpicosecond kinetics for photodissociated hemes are independent of the protein matrix (*10*). These findings plus the observed constancy of the transient absorption spectrum from picoseconds to nanoseconds after photolysis (*8*) support the idea that deoxy Hb* (5 psec $< t <$ 20 nsec) contains a deoxy heme with a displaced iron. Aside from accommodating the motion of the iron, the protein structure is virtually unrelaxed with respect to the ligated configuration. The nanosecond spectra reflect this transiently frozen geometry of the deoxy Hb*. The difference in ν_{Fe-His} between R- and T-state Hb* (10 nsec) arises from tilt or other strain-induced variations in the distance between the imidazole carbon and the pyrrol nitrogen. As long as the iron is sufficiently displaced out of the heme plane, the localized energy difference between the tilted and untilted geometry is small (see Fig. 6). However, the repulsive force increases substantially for the tilted configuration when the iron moves into the heme plane (*48*). It follows that it is energetically more costly to move the iron into the heme plane for the tilted species. The tertiary structure–dependent difference in this energy corresponds to δ (Fig. 3).

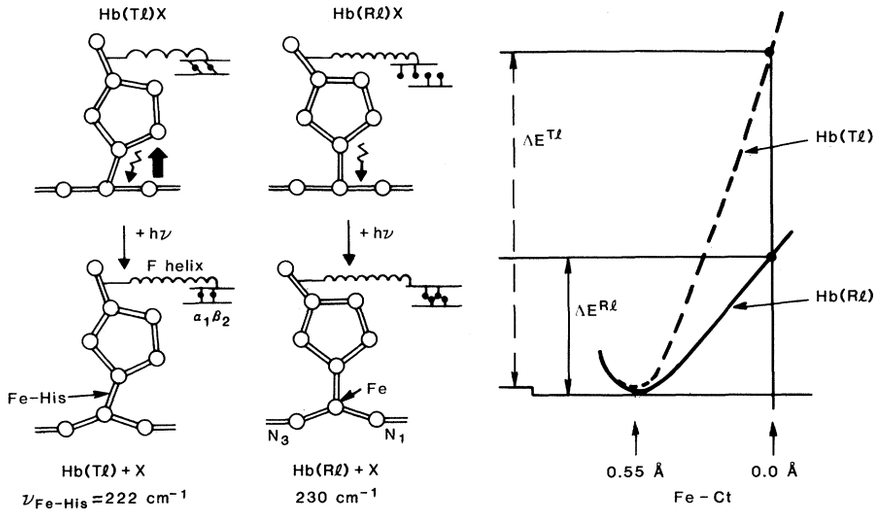

Fig. 6. The proposed relation between the tilt of the proximal histidine and the tertiary structure of the heme pocket for R- and T-state ligated Hb's. The right side of the figure shows how the tilt could affect the energetics of ligand binding. When the iron is out of the heme plane, there is only a small energy difference between the configurations having different tilts whereas decreasing the iron to heme center (Fe-Ct) distance generates a large difference due to the enhanced nonbonded interactions associated with the tilted configuration. This interaction generates a torque upon the histidine that counters the tilt. The differences between the ΔE values contributes to both δ and δ* in Fig. 3.

X-ray data indicate a strong coupling through the F helix between the proximal histidine (F8) and the α_2-β_2 interface. Thus the F helix can function as a conduit through which strain can shuttle back and forth between the iron (via the histidine) and the α_1-β_1 interface. For a deoxy heme, the out-of-plane iron induces minimal strain regardless of the quaternary structure (Fig. 6). The orientation of the proximal histidine is determined by the pull of the F helix, which is generated by the α_1-β_2 interface. The more T-like the interface, the greater the pull on the histidine and hence the greater the tilt. The torque upon the histidine (Fig. 6) that is set up upon ligation counters this pull and at the same time causes strain to be transmitted through the F helix to the interface. Thus we have a feedback loop that is analogous to the allosteric core of Karplus and coworkers (*47*). The F helix–mediated pull of the interface provides the frictional drag or resistance that gives rise to δ and δ* (see Fig. 3). The greater this pull, the greater the counter pull generated by the ligation-induced torque on the histidine (Fig. 6). The counter strain generated by the torque destabilizes the interface and in the case of HbA leads to a change in quaternary structure (T → R). The new R-state interface is sustained by the pull from the ligated heme-histidine unit. Associated with the inherently less stable R-state interface unit is a reduction in the pull on the histidine. One can readily tune such a system by modifying the properties of the interface via evolution and solution conditions.

Conclusions

Two spectroscopically distinguishable tertiary structures are evident in the heme pocket of both the R- and T-state quaternary structures of Hb's derived from a large variety of animal sources. Within each quaternary structure ligation induces changes in the environment of the heme that transforms the deoxy R- or T-state heme pocket [designated as Hb(Rd) or Hb(Td), respectively] to the ligated R- or T-state heme pocket [Hb(Rℓ) or Hb(Tℓ), respectively]. The frequency of the ν_{Fe-His} associated with the electronically relaxed deoxy heme increases in going from Hb(Td) to Hb(Tℓ) ≈ Hb(Rd) to Hb(Rℓ). With respect to a deoxy heme, only Hb(Td) represents an equilibrium species for HbA. By following the evolution of ν_{Fe-His} subsequent to the photolysis of COHb(Rℓ), one can demonstrate that the initial photo product is Hb(Rℓ) but relaxes with a solution-dependent rate to Hb(Rd) prior to the R-T switch. The functional significance of this solution-dependent relaxation is indicated by virtue of the involvement of ν_{Fe-His}. Studies have revealed a correlation between geminate recombination and the structural determinants of ν_{Fe-His}. These stud-

ies allow for a distinct reaction coordinate diagram to be associated with each value of ν_{Fe-His}. The relaxation experiments indicate that the potential surface controlling ligand bonding can change on the time scale of geminate recombination. On the basis of these findings, a model is described incorporating both sequential and parallel processes that can account for species-specific and solution-dependent variations in ligand reactivity within a given quaternary state.

Note added in proof: In recent studies we have measured both the picosecond geminate rebinding of O_2 in a large variety of vertebrate hemoglobins (*49*) and the corresponding time-resolved, low-frequency Raman spectra of the deoxy photoproduct occurring within 25 psec of photodissociation (*50*). These studies reveal that the values of ν_{Fe-His} in the 25-psec transients are the same as in 10-nsec transients discussed here and that the yield for the picosecond geminate rebinding correlates with the ν_{Fe-His} values of the associated deoxy transients. These results confirm the conclusions expressed in this article regarding the correlation between the geminate yield and ν_{Fe-His} that were inferred from the nanosecond studies.

References and Notes

1. Certain species of Antarctic ice fish have no hemoglobin.
2. M. F. Perutz, *Proc. R. Soc. London Ser. B* **208**, 135 (1980).
3. R. G. Shulman, J. J. Hopfield, S. Ogawa, *Q. Rev. Biophys.* **8**, 325 (1975).
4. A. DeYong, R. P. Pennelly, A. L. J. Wilson, R. W. Noble, *J. Biol. Chem.* **251**, 6692 (1976); L. D. Kwiatowski and R. W. Noble, *ibid.* **257**, 8891 (1982).
5. J. M. Baldwin and C. Chothea, *J. Mol. Biol.* **129**, 175 (1979).
6. L. J. Noe, W. G. Eisert, P. M. Rentzepis, *Proc. Natl. Acad. Sci. U.S.A.* **75**, 573 (1978); A. H. Reynolds, S. D. Rand, P. M. Rentzepis, *ibid.* **78**, 2292 (1981).
7. B. I. Greene, R. M. Hochstrasser, R. B. Weisman, W. A. Eaton, *ibid.* **75**, 5255 (1978).
8. D. A. Chernoff, R. M. Hochstrasser, A. W. Steele, *ibid.* **77**, 5606 (1980).
9. J. A. Hutchinson, T. G. Traylor, L. J. J. Noe, *J. Am. Chem. Soc.* **104**, 3321 (1982).
10. J. L. Martin *et al.*, *Proc. Natl. Acad. Sci. U.S.A.* **80**, 173 (1983); J. L. Martin *et al.*, *Biochim. Biophys. Res. Commun.* **107**, 803 (1982).
11. K. B. Lyons and J. M. Friedman, in *Hemoglobin and Oxygen Binding*, C. Ho, Ed. (Elsevier, New York, 1982), p. 333.
12. L. Lindqvist, S. El Mohsni, F. Tfibel, B. Alpert, *Nature (London)* **288**, 729 (1980).
13. C. Sawicki and Q. H. Gibson, *J. Biol. Chem.* **251**, 1533 (1976).
14. J. Hofrichter *et al.*, *Proc. Natl. Acad. Sci. U.S.A.* **80**, 2235 (1983).
15. J. M. Friedman *et al.*, *J. Biol. Chem.* **258**, 10564 (1983).
16. T. G. Spiro, *Isr. J. Chem.* **21**, 81 (1981).
17. S. A. Asher, *Methods Enzymol.* **76**, 371 (1981).
18. J. M. Friedman, D. L. Rousseau, M. R. Ondrias, *Annu. Rev. Phys. Chem.* **33**, 471 (1982).
19. D. L. Rousseau and M. R. Ondrias, *Annu. Rev. Biophys. Bioeng.* **12**, 357 (1983).
20. J. M. Friedman, R. A. Stepnoski, R. W. Noble, *FEBS Lett.* **146**, 278 (1982).
21. J. M. Friedman, D. L. Rousseau, M. R. Ondrias, R. A. Stepnoski, *Science* **218**, 1244 (1982); J. M. Friedman, in *Time-Resolved Vibrational Spectroscopy*, G. Atkinson, Ed. (Academic Press, New York, 1983), p. 307.
22. J. A. Shelnutt, D. L. Rousseau, J. M. Friedman, S. R. Simon, *Proc. Natl. Acad. Sci. U.S.A.* **76**, 4409 (1979).
23. J. M. Friedman *et al.*, *Biochemistry* **21**, 2022 (1982).
24. T. G. Spiro and J. M. Burke, *J. Am. Chem. Soc.* **98**, 5482 (1976); M. Tsubaki, K. Nagai, T. Kitagawa, *Biochemistry* **19**, 379 (1980).
25. M. R. Ondrias, D. L. Rousseau, S. R. Simon, *J. Biol. Chem.* **258**, 5638 (1983); M. R. Ondrias, J. M. Friedman, D. L. Rousseau, *Science* **220**, 615 (1983).
26. G. N. Lapennas and P. Lutz, *Respir. Physiol.* **48**, 59 (1982); P. Lutz and G. N. Lapennas, *ibid.*, p. 75; P. Lutz, in *A Companion to Animal Physiology* (Cambridge Univ. Press, Cambridge, 1982), p. 65.
27. S. Matsukawa, K. Mawataii, Y. Yoneyama, T. Kitagawa, *J. Am. Chem. Soc.*, in press.
28. R. H. Austin *et al.*, *Biochemistry* **14**, 5355 (1975); L. Eisenstein and H. Frauenfelder, in *Biological Events Probed by Ultrafast Laser Spectroscopy*, R. R. Alfano, Ed. (Academic Press, New York, 1982), p. 321.
29. D. D. Dlott *et al.*, *Proc. Natl. Acad. Sci. U.S.A.* **80**, 6329 (1983).
30. D. A. Duddell, R. J. Morris, J. T. Richards, *Chem. Commun.* **1979**, 75 (1979); B. Alpert, S. E. Mohsni, L. Lindqvist, F. Tfibel, *Chem. Phys. Lett.* **64**, 11 (1979).
31. J. M. Friedman and K. B. Lyons, *Nature (London)* **284**, 570 (1980).
32. P. A. Cornelius, R. M. Hochstrasser, A. W. Steele, *J. Mol. Biol.* **163**, 119 (1983).
33. H. Roder *et al.*, *Proc. Natl. Acad. Sci. U.S.A.*, in press.
34. T. W. Scott and J. M. Friedman, *J. Am. Chem. Soc.* **106**, 5677 (1984).
35. W. Doster *et al.*, *Biochemistry* **21**, 4831 (1982).
36. R. J. Morris and Q. H. Gibson, *J. Biol. Chem.* **255**, 8050 (1980).
37. E. R. Henry, J. H. Sommer, J. Hofrichter, W. A. Eaton, *J. Mol. Biol.* **166**, 443 (1983).
38. C. A. Sawicki and Q. H. Gibson, *J. Biol. Chem.* **254**, 4058 (1979); R. J. Morris and Q. H. Gibson, *ibid.* **259**, 365 (1984).
39. T. W. Scott, J. M. Friedman, V. Macdonald, *J. Am. Chem. Soc.*, in press.
40. N. Alberding *et al.*, *Biochemistry* **17**, 43 (1978).
41. T. G. Traylor *et al.*, in *Hemoglobin and Oxygen Binding*, C. Ho, Ed. (Elsevier, New York, 1982), p. 425.
42. A. Szabo, *Proc. Natl. Acad. Sci. U.S.A.* **75**, 2108 (1978).
43. T. W. Scott, J. M. Friedman, M. Ikeda-Saito, T. Yonetani, *FEBS Lett.* **158**, 68 (1983).
44. N. Agmon and J. J. Hopfield, *J. Chem. Phys.* **79**, 2042 (1983).
45. J. M. Friedman, S. R. Simon, T. W. Scott, *Copeia*, in press.
46. R. J. Morris and Q. H. Gibson, *J. Biol. Chem.* **275**, 4869 (1982).
47. B. R. Gelen and M. Karplus, *Proc. Natl. Acad. Sci. U.S.A.* **74**, 801 (1977); B. R. Gelin, A. W.-M. Lee, M. Karplus, *J. Mol. Biol.* **171**, 489 (1983).
48. B. D. Olafson and W. A. Goddard III, *Proc. Natl. Acad. Sci. U.S.A.* **74**, 1315 (1977); W. A. Goddard and B. D. Olafson, in *Biochemical and Chemical Aspects of Oxygen*, W. Caughy, Ed. (Academic Press, New York, 1979), p. 87.
49. J. M. Friedman *et al.*, *Science*, in press.
50. E. W. Findsen *et al.*, in preparation.

51. Much of the work described in this article was conducted in collaboration with T. W. Scott, R. Stepnoski, M. Ondrias, D. Rousseau, S. Simon, K. B. Lyons, and V. Macdonald. Their respective contributions are gratefully acknowledged.

RESEARCH ARTICLE

The Mechanism of Irreversible Enzyme Inactivation at 100°C

Tim J. Ahern and Alexander M. Klibanov

As the temperature is increased, all enzymes eventually lose their catalytic activity. This thermal inactivation of enzymes may be either reversible or irreversible, depending on whether return to ambient temperature results in the return of enzymatic activity within a reasonable period of time (*1*). Reversible thermal inactivation (denaturation) of enzymes is caused by temperature-induced conformational transitions in the protein molecule; this phenomenon has been extensively studied and its mechanisms are well understood (*2–5*). The pathways and mechanisms of irreversible thermoinactivation of enzymes, however, remain obscure, primarily because of severe conceptual and experimental problems encountered in their investigation. Knowledge of these mechanisms is essential for the development of rational approaches to enzyme stabilization (*1, 6*), with special application to protein engineering (*7*) and to the enhancement of enzyme thermostability (*8*).

A number of chemical reactions can take place in proteins at high temperature, especially at extremes of *p*H (*9*). But little is known concerning the processes that actually lead to enzyme inactivation in the *p*H range of relevance to enzymatic catalysis (*p*H 4 to 8) and their relative effects. We therefore undertook the following study.

We used hen egg-white lysozyme as a model because it is a small monomeric enzyme containing no nonprotein components and its structure and properties have been thoroughly investigated (*10*).

Tim J. Ahern is a postdoctoral associate and Alexander M. Klibanov is associate professor of applied biochemistry in the Department of Applied Biological Sciences, Massachusetts Institute of Technology, Cambridge 02139.